Coupled Systems Mechanics, *Vol. 10, No. 3 (2021) 263-280*
DOI: https://doi.org/10.12989/csm.2021.10.3.263

Viscoelastic behavior of concrete structures subject to earthquake

Rosa Adela Mejia-Nava*[1], Adnan Ibrahimbegovic[1,2a],
Norberto Domínguez-Ramírez[3b] and Esteban Flores-Méndez[3c]

[1]*Université de Technologie Compiégne, Laboratoire Roberval of Mechanics, France*
[2]*Chair of Computational Mechanics UTC and UF Institut Universitaire de France, France*
[3]*Postgraduate Studies and Research Section, ESIA-UZ, Instituto Politécnico Nacional, Mexico*

(Received May 22, 2021, Revised May 28, 2021, Accepted June 4, 2021)

Abstract. This paper investigates an alternative way to the Raleigh formula to catch con- tributions of damping effects. Nowadays, thanks to the power of new software and effi- cient computational methods, there exist possibility to implement new analysis of damping through multiscale approach. The corresponding homogenization of a representative elemen- tal volume of concrete is used to calculate the effective properties of the composite, since energy dissipation properties such as viscoelasticity are not taken into account. At the end of this work, these methodologies are incorporated into a column of a building subject to seismic action. More precisely, with concrete as a composite material (aggregate+cement), we can use homogenization methods to calculate its effective properties by using the classical approach of a representative elemental volume. This can help to take into account properties of energy dissipation, such as produced by viscoelasticity. Finally, for illustration, the pro- posed methodology is applied to structural analysis of a column under the most unfavorable conditions in a building subject to earthquake action.

Keywords: damping; viscoelastic; homogenization; multiscale

1. Introduction

In the dynamic analysis of structures, damping has a very important role as it is directly related to the dissipation of energy during an earthquake. At the present, it is difficult to quantify damping, as it is considered proportional to the mass and stiffness of the system (Rayleigh damping). Based on this hypothesis, simplified models have been formulated, employing a damping ratio associated with the type of material: 5% for concrete and 2% for steel. However, with the need to make more realistic assessments and predictions of structural response to earthquakes, it is necessary to reformulate the concept of damping depending on the mechanical properties of materials as well as different mechanisms of dam- age that can be activated. In the reformulation context, which will be presented damping, is a function of a nonlinear dissipative phenomenon. This work presents a multi-

*Corresponding author, Ph.D., E-mail: rosa-adela.mejia-nava@utc.fr
[a]Professor, E-mail: adnan.ibrahimbegovic@utc.fr
[b]Professor, E-mail: ndominguez@ipn.mx
[c]Professor, E-mail: efloresm@ipn.mx

http://www.techno-press.org/?journal=csm&subpage=8 ISSN: 2234-2184 (Print), 2234-2192 (Online)

scale strat- egy computation that incorporates not only the visco-elastic effects in the overall concrete structural damping system under earthquake but also calculates the mechanical parameters (Young's modulus) from the heterogeneity of the material. By considering that concrete is a non-homogeneous material, mainly composed of cement and fine and coarse aggregate. Bearing in mind that cement and fine aggregate have more viscous properties than coarse aggregate, at the mesoscale it is intended to apply different methods of homogenization to obtain the mechanical properties of a representative volume element (RVE) of concrete. The issue of homogenization result for elasticity modulus is the most classical; namely, the lower and upper bound of Reuss and Voigt can be averaged is order to provide the improved value of elasticity module. Similar path has to be followed for quantifying the contribution of viscosity to damping effects. Preliminary results show that the heterogeneity can induce significant changes in the mechanical parameters of the material, and therefore have an effect on the structural response of the system (e.g., Clough and Penzien 1995, Abbas *et al*. 2014). The strategy applied in this research was the following: first, an alternative methodology is proposed to obtain the damping matrix of a structure, in a similar way to the stiffness matrix of each element, applying multiscale methodology based on the heterogeneity of the material to obtain the mechanical parameters (modulus of elasticity and coefficient of viscosity). Then the adequate finite element mesh of a representative volume element (RVE) of concrete is established, taking into account that there are two different materials: cement and sand which form the RVE matrix, while the coarse aggregate is modeled as a single inclusion. In this model, the bounds of Reuss and Voigt, along with standard homogenization method are applied to obtain an average Young's Modulus. Finally, an illustrative example of concrete frame structure under earthquake was presented, with modeling and design carried out in agreement with the standard engineering design code. Once the calculation was done a critical column was chosen. On the top of the column displacements that were caused by an earthquake were imposed. The column was modeling independently incorporating the viscoelastic effects in the material first with a rectangular finite element mesh and later with the RVE. Finally, the stress versus deformation curves were obtained from the two analyzes and presented.

2. Preliminary remarks on current approach to dynamics

2.1 Rayleigh formula

The currently dominant approach in engineering practice when studying dynamic vibra- tion of engineering structures or systems relies upon well-known equations of motion (e.g., Clough and Penzien 1995, Ibrahimbegovic and Ademovic 2019). For forced vibrations of an undamped system, the equations of motion can be written in the form

$$M\ddot{u} + C\dot{u} + Ku = f(t) \tag{1}$$

where M and K are structure mass and stiffness matrix respectively, $F(t)$ is applied dynamic force (e.g., earthquake, wind, explosions, etc.) and $u(t)$ is the corresponding dynamic response. The main advantage of such an approach is that it allows for very efficient computations by applying the classical mode superposition approach (e.g., Clough and Penzien 1995, Chopra 2014) where the equations of motion are uncoupled in terms of modal response (representing the motion of a complex structure in a particular mode of free vibrations) and solved easily, either analytically or numerically, (e.g., Ibrahimbegovic 2009). Each equation is solved independently. The critical damping value is

$$C_c = 2m\omega \quad (2)$$

To evaluate the response, it is convenient to express the damping in terms of the damping ratio, which is given by

$$\xi = \frac{c}{C_c} = \frac{c}{m\omega} \quad (3)$$

In order to account for damped vibrations (which certainly corresponds to reality, since the vibrations eventually stop due to different energy dissipation mechanisms), one then uses the well-known Rayleigh damping (e.g., Clough and Penzien 1995, Ibrahimbegovic and Ademovic 2019). The latter assumes that the damping phenomena are proportional to vibration velocities, with the coefficient of proportionality, so-called damping matrix C, that can be constructed as a linear combination of mass and stiffness matrix

$$\mathrm{C} = \mathrm{M}a_0 + \mathrm{K}a_1 \quad (4)$$

where two coefficients, or Rayleigh parameters α and β, are obtained from the chosen damping coefficient ξ that characterize a typical attenuation of vibration amplitudes with typical choices of 5 % for concrete and 2% for steel structures; see Ibrahimbegovic and Ademovic (2019) on how to simply obtain the Rayleigh parameters according to

$$\begin{pmatrix} a_0 \\ a_1 \end{pmatrix} = \frac{2\xi}{\omega_n + \omega_m} \begin{pmatrix} \omega_n \omega_m \\ 1 \end{pmatrix} \quad (5)$$

where ω_n is the chosen frequency that should be damped with precisely the chosen amount of damping. Given the two Rayleigh parameters, further improvement can be done by choosing two different frequencies ω_n and ω_m while making sure that the chosen damping coefficients would precisely apply to those two modes. However, one has to realize that all other frequencies would be damped in a way that is quite unrealistic, either somewhat less (inside the interval between chosen frequencies) or much more, see Fig. 1 for illustration (Ibrahimbegovic and Ademovic 2019).

2.2 What we propose as a more material-scale-base damping model for dynamics capable of representing different phases of dynamic response

In this paper, we seek to construct and develop a very new damping concept obtained from

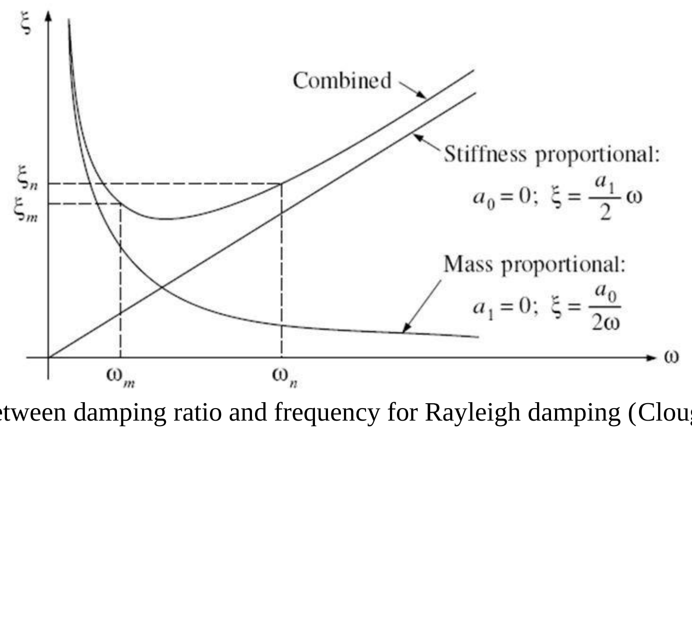

Fig. 1 Relationship between damping ratio and frequency for Rayleigh damping (Clough and Penzien 1995)

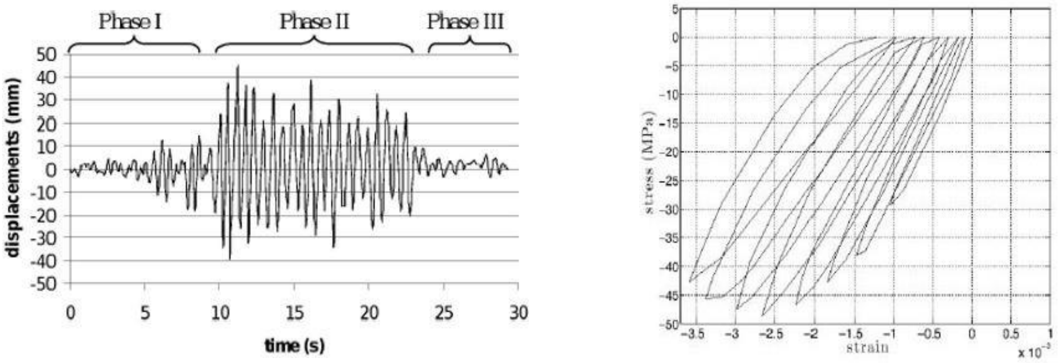

(a) Three damping phases (b) Experimental result for cyclic behavior of concrete

Fig. 1 Mesh grid of topographic model

material scales, which can provide a much better correlation with the dynamics response of real-life structures, under complex loading such as earthquakes. More precisely, a very typical response to earthquake (see Fig. 2) passes through three different phases: i) small vibration amplitudes for mild earthquake, ii) strong shaking with large vibration amplitudes for the dominant phase of earthquake excitation, and iii) free vibrations of the damaged structure produced by an earthquake.

At the same time to take into account the material homogenization it is necessary to in- corporate energy dissipation characteristics such as viscoelasticity, damage, plasticity, and others (see Ibrahimbegovic *et al.* 2014a, Lee *et al.* 1999).

Hybrid-stress formulation gives us the possibility to compute the inverse of the stiffness matrix, where the effects of plasticity and damage mechanisms are uncoupledIbrahimbegovic, Mejia-Nava (2021). Hybrid-stress formulation is based upon the consistent variational formulation, which allows constructing independent discrete approximation for stresses and displacements. In this way, we can obtain the inverse of the stiffness matrix or elasto-visco- plastic-damage compliance. The advantage of the inverse of the stiffness matrix for plasticity and damage is that we can keep each energy-dissipation mechanism uncoupled from each other, which allows to integrate them in the most efficient manner; see Ibrahimbegovic, Mejia-Nava (2021).

2.3 Multiscale modeling

Due to their macroscopic nature, current models have difficulties in correctly describing the physical mechanisms (mechanisms of fracture, damage, and transport) that take place on finer scales and that involve macroscopic observations (see Ibrahimbegovic and Papadrakakis 2010, Marenic *et al*. 2012, Markovic *et al*. 2005). Emphasizing that the objective is to study the phenomenon of damping in concrete, it is considered that it is possible to study it as a multiscale phenomenon. With this type of approach, the phenomenological models are replaced by refined models of inelastic behavior built on two scales: macroscale that repre- sents the homogenized behavior of the material for the computation of the response of the global structure, and the microscale that allows us to capture fine details of microstructure by multiple heterogeneous phases of the materials (see Fig. 3). The advantage of this type of approach is that it offers a more realistic interpretation of the mechanisms of inelastic behavior (see Rukavina *et al*. 2019, Rukavina *et al*. 2019). From this perspective, multi-scale strategies seek to establish a (numerical) link between the initial constituent

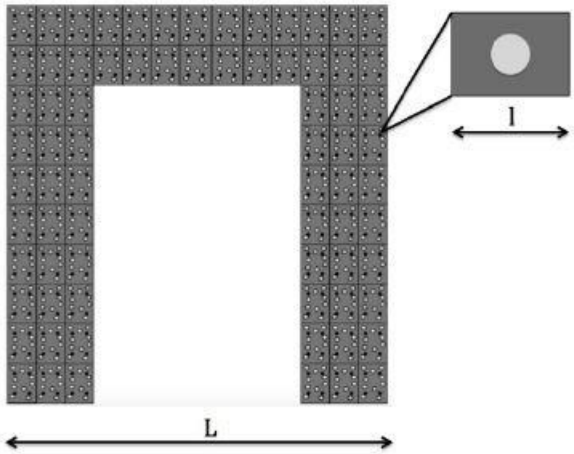

Fig. 3 Macro-scale and micro-scale model

(a) Maxwell Model (b) Kelvin-Voigt model

Fig. 4 Mechanical representation of viscous and elastic behavior

properties and the resulting mechanical properties on a macro scale. A bridge of this type would require, on the one hand, a very precise and exact description of the microstructure of the material exhibiting various phases and, on the other hand, the ability to use such a description in ad-hoc numerical methods such as, for example, a finite element model (see Benkemoun *et al*. 2012). The way which should be followed for the modeling of a strutural system inspired by multi-scale strategies consists of: first, obtain the elastic behavior with the micro-scale modeling where the homogenized modulus of elasticity and the viscous behavior can be obtained separately, obtain the viscosity constant, and finally couple this with the global structure on the macro-scale that represents the homogenized behavior of the material.

2.4 Linear viscoelastic behavior

The viscoelastic behavior of materials lies somewhere between the viscosity for Newton's fluids and Hooke's elastic solids. The first are generally fluids in which the resistance to shear stress tends to zero or is zero. Therefore when applying a load, its deformations become unlimited, and once it is removed, it does not show recovery from its deformation. The latter are those, when applying the load there are limited deformations, and when removing the load the solid returns to its original state. Ideally, a material with viscoelastic behavior recovers all of the deformations that it acquires after the application of a load (see Ibrahimbegovic 2009). The best-known mechanical representations of viscoelastic behavior are Kelvin's scheme and Maxwell's scheme as follow.

The following shows the formulation used in the finite element program (FEAP) for a viscoelastic material. The stresses and strains for a linear viscoelastic material can be expressed as follows

$$\sigma = s + \mathrm{m}P \tag{6}$$

$$\epsilon = e + \frac{1}{3}\mathrm{m}\theta \tag{7}$$

where σ are the Cauchy stresses, s is the deviating stress, P is the principal stress ϵ is the deformation, e it is the deviatoric strain, and θ is the corresponding volume change. Linear viscoelastic behavior is represented in a differential equation or integral form of the equation. In the differential equation of the constitutive model, the behavior can be characterized as

$$\mathrm{P(s)} = 2\mathrm{GQ(e)} \tag{8}$$

where P and Q are differential operators expressed as

$$\mathrm{P} = \mathrm{p}_m \frac{\vartheta^m}{\vartheta t^m} + \mathrm{p}_{m-1} \frac{\vartheta^{m-1}}{\vartheta t^{m-1}} + \cdots + \mathrm{p}_0 \tag{9}$$

$$\mathrm{Q} = \mathrm{q}_m \frac{\vartheta^m}{\vartheta t^m} + \mathrm{q}_{m-1} \frac{\vartheta^{m-1}}{\vartheta t^{m-1}} + \cdots + \mathrm{q}_0 \tag{10}$$

$$\mathrm{G} = \frac{E}{2(1-v)} \tag{11}$$

G is identical to the elastic shear modulus, the operator s can be written as

$$\mathrm{s} = 2\mathrm{G}\left(\mu_0 \mathrm{e} + \textstyle\sum_{i=1}^{N} \mu_i q^i\right) \tag{12}$$

This form of representation is equivalent to a generalized Maxwell model (a set of Maxwell's models in parallel). The set of first-order differential equations can be integrated for specific deformations e. The integral for each term is given by the homogeneous differential equation

$$q^i(\mathrm{t}) = \int_{-\propto}^{t} e^{-\frac{t-\tau}{\lambda_i}}\, \dot{e}(\tau) d\tau \tag{13}$$

The relaxation modulus function is defined in terms of an idealized experiment in which at time zero (t=o), a specimen is subject to a strain constant e_0, and the stress response is recorded, $s(t)$. In this way, a unique relationship is obtained that is independent of the magnitude of the applied stress. This relationship can be written as

$$s(\mathrm{t}) = \int_{-\propto}^{t} \mathrm{G}(t-\tau)\dot{e}(\tau) d\tau \tag{14}$$

It can be seen that the above formula is a generalization of Maxwell's model. In fact, the form of the integral equation can be defined as a generalization of the Maxwell model, assuming the relaxation of the shear modulus in the form of the Prony series (see Taylor 2008)

$$G(\mathrm{t}) = \mathrm{G}\left(\mu_0 + \textstyle\sum_{i=1}^{N} \mu_i e^{\frac{-t}{\lambda_i}}\right) \tag{15}$$

Where

$$\mu_0 + \textstyle\sum_{i=1}^{N} \mu_i = 1 \tag{16}$$

With this form, the integral equation is identical to the model of the differential equation for the generalized Maxwell model.

2.5 Homogenization theory

At the micro-scale level, it is important to take into account aspects such as the heterogeneity of the material at the microstructural scale. In the case of concrete, it is a mixture of cement, gravel, sand, and water, which goes through a process of setting and hardening; the aggregates represent between 60% to 70% of the total volume of concrete, these aggregates have different properties, therefore, the contribution to the dissipation of the forces to which it is subjected is different for each type of material. With the homogenization method, we can obtain a representative value, consistent with the properties of the materials. The modelling of the inelastic behaviour of heterogeneous materials is strongly related to the scale of observation. From a macro-scale point of view, the usual engineering approach considers most of these materials as homogeneous (see Benkemoun *et al*. 2012). In the classic problem of homogenization, where the macro and micro scales do not necessarily have permanent communication, we can carry out a separate analysis, and establish the properties averaged on the micro-scale. The micro-scale analysis is done by studying the so-called Representative Elemental Volume (RVE) in order to identify the best adequate phenomenological model of constitutive behavior capable of representing all the pertinent details of the inelastic behaviour of a given material (see Ibrahimbegovic 2009). In the case of elastic homogenization with an inclusion, two theories can be combined: the Reuss homogenization used to obtain a minimum modulus of elasticity as follows

$$E_{min} = \frac{\delta_M^2}{2w} \tag{17}$$

Where

$$\delta_M = \frac{1}{V}\sum_{i=1}^{ei} \mathrm{A}_i^{el}\delta_i^m \tag{18}$$

Similarly, the Voigt homogenization (see Eq. (17)) used to obtain a maximum modulus of elasticity

$$E_{min} = \frac{2w}{\varepsilon_M^2} \tag{19}$$

Where

$$\varepsilon_M = \frac{1}{V}\sum_{i=1}^{ei} \mathrm{A}_i^{el}\varepsilon_i^m \tag{20}$$

With both, we can find an average modulus of elasticity, increase the growing volume percentages of Emax and Emin until reaching the same value. This value is substituted into the constitutive Kelvin equation for viscoelastic behavior. According to the variation of the total energy of the potential, we have that the double of this energy is equal to the sum of the efforts by the deformations by the area between the total volume as follow

$$2w = \frac{1}{V}\sum_{i=1}^{\theta i}(\delta_{11}^m\varepsilon_{11}^m + \delta_{22}^m\varepsilon_{22}^m + \delta_{33}^m\varepsilon_{33}^m + \delta_{12}^m\varepsilon_{12}^m)\, A_{el} \tag{21}$$

3. Numerical examples

3.1 Homogenization

In order to illustrate how to apply the homogenization theory, we conducted an example for a

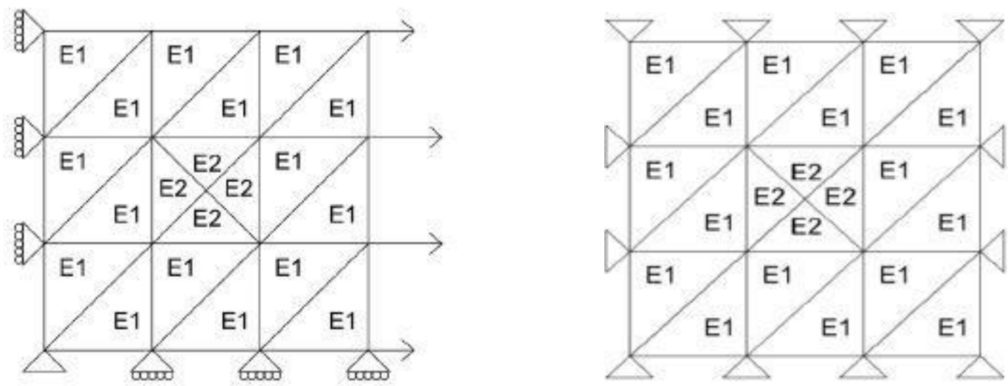

(a) RVE Reuss (b) RVE Voigt

Fig. 5 Meshes of a representative elemental volume

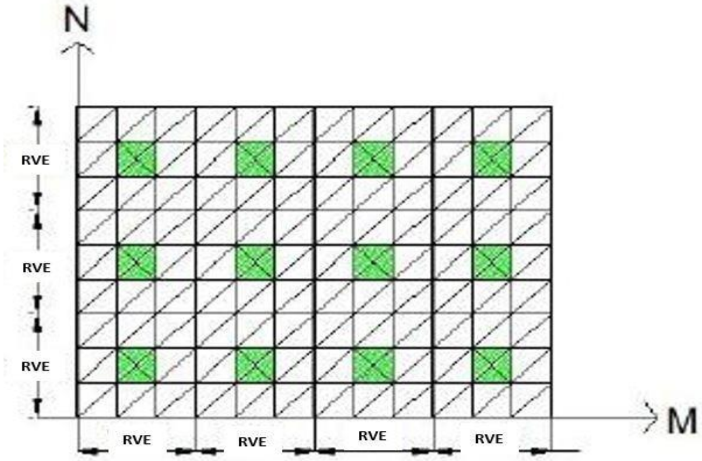

Fig. 6 Mesh with multiple RVEs, with homogeneous distribution

concrete building. The first step to analyze an RVE is to find the appropriate mesh to represent the material, which in this case is concrete, consisting of cement and aggregate as two different materials. The size of the RVE depends on the homogenized equivalent properties, the minimum aggregate size being 4.75 mm and the maximum being 90 mm. In this case, the aggregate size was taken as 50 mm, leading to the matrix of size 150 mm×150 mm. The chosen mesh is represented in Fig. 5 where the domain is made up of two materials having a different modulus of elasticity, distributed as shown in Fig. 5: material 1 represents cement, with the modulus of elasticity E_1=10 GPa, and material 2 represents the coarse aggregate with modulus elasticity E_2=70 GPa.

In order to obtain a correct modulus of elasticity of the material, it is necessary to elaborate a set of regions made up of a certain number of RVE meshes, increasing the number of RVE in both directions vertically (N) and horizontally (M) as follows.

Finite Element Analysis Program (FEAP) was used to obtained the results for Reuss and Voigt models (see Fig. 7) using one Representative Elemental Volume. The following results were obtained.

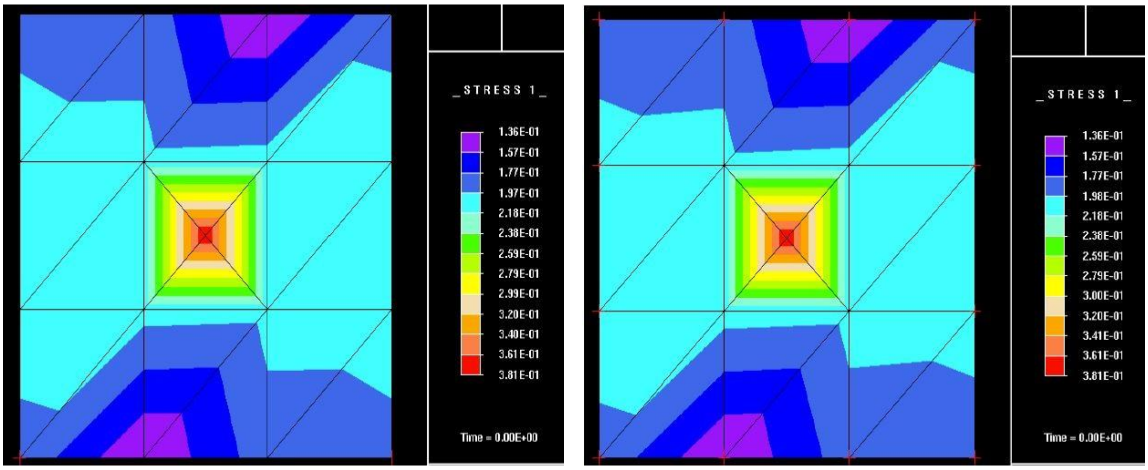

(a) E_{min}=12.5618 (b) E_{max}=12.8091

Fig. 7 Results with FEAP

Table 1 Homogenization results

Model	*M*	*N*	E_{min} (GPa)	E_{max} (GPa)	Difference
1	1	1	12.5618	12.8091	0.2473
2	2	1	12.6116	12.8227	0.2111
3	10	5	12.6702	12.8358	0.1656
4	20	10	12.6767	12.8364	0.1597
5	30	15	12.6790	12.8367	0.1577
6	40	20	12.6800	12.8366	0.1566
7	50	25	12.6806	12.8366	0.1560
8	60	30	12.6810	12.8366	0.1556
9	70	35	12.6813	12.8366	0.1553
10	80	40	12.6815	12.8366	0.1551
11	90	45	12.6817	12.8366	0.1549
12	100	50	12.6818	12.8366	0.1548
13	110	55	12.6819	12.8366	0.1547

Thirteen models were tested. The dimensions in *M* and *N* (see Fig. 6) are shown in Table 2.1 as well as the values obtained for the maximum and minimum modulus of elasticity, and the difference between them is shown in the last column.

In Fig. 6 we can see how E_{max} stabilizes at a value of 12.8. The initial difference of E_{max} with respect to E_{min} is 24%. The value that is changing is E_{min} and it is approaching the already stabilized value of 12.8. It has a variation with respect to the values of a single RVE, as the starting difference was 15%.

3.2 Practical applications

To evaluate the proposed strategy, in the first stage a building was designed (see Figs. 9 and 10), and then the structure was exposed to an earthquake. It is a concrete frame structure with secondary

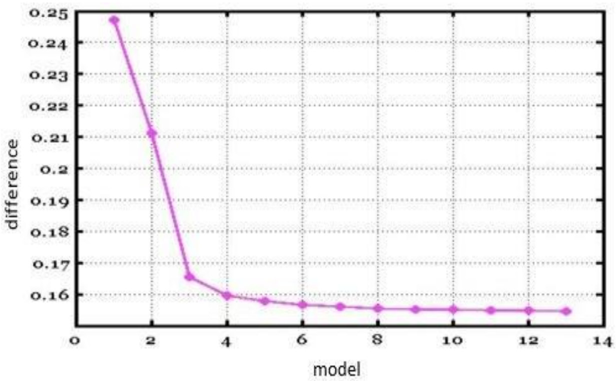

Fig. 8 Homogenization results difference between E_{max} and E_{min}

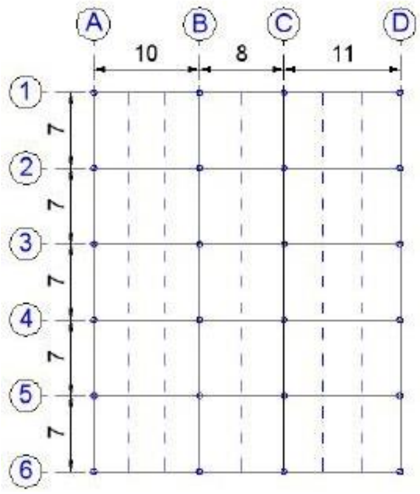

(a) First level

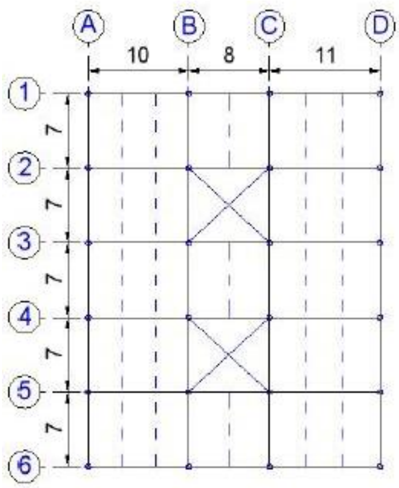

(b) Second level

Fig. 9 Geometry in the construction plant

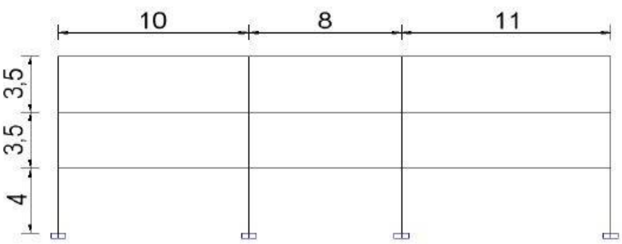

Fig. 10 Structure elevation

beams located in an unfavorable direction. The buildings consist of 3 floors, the first with a height of 4 m and the other two of 3.5 m. The construction concept pertains to column supported slabs, that are weakened by the holes at the second and third story levels. Concrete quality of $f'c$=350 kg/cm^2 was used for each frame components (longitudinal girders, transverse girders, secondary girders and square columns) and for the slab $f'c$=250 kg/cm^2, while for the reinforcing steel of the

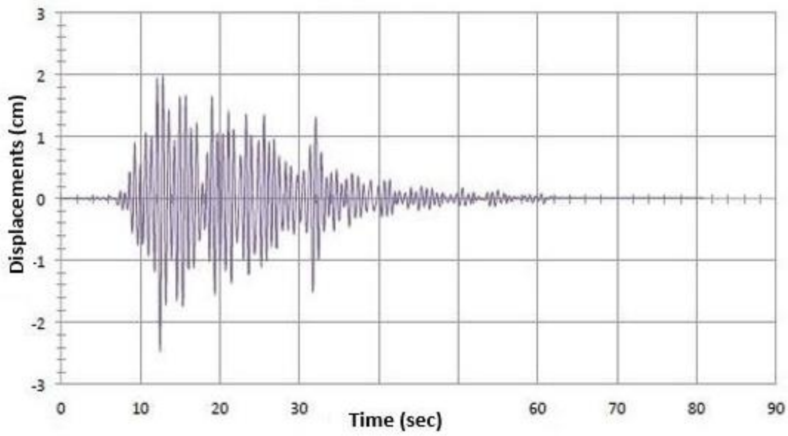

Fig. 11 Critical column superior displacements

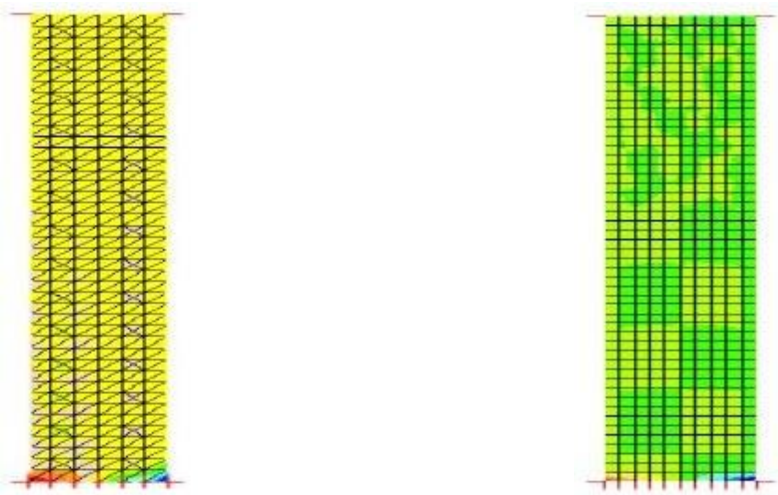

(a) Mesh column RVE (b) Rectangular mesh column

Fig. 12 Geometry in the construction plant

entire structure grade $f'c$=4200 kg/c m^2 was applied.

Once the results were obtained and analyzed the most critical column was chosen. In Fig. 11 the displacements in time of the most unfavorable column are shown. The maximum displacement of 1.95504 cm is reached at 12.8 seconds, and in the case of the minimum or negative displacement, the displacement is -2.44647 cm which was reached at 12.5 seconds.

For the structural analysis performed subsequently, we chose the column having the most unfavorable conditions with respect to the given loading and structural elements. In this case, it was column 5C (see Fig. 9). First, homogenization analysis was performed by taking into account different characteristics of the material. Based on this choice, we make two different analyses: i) first with viscoelastic material, by studying the parameters that can affect the behavior of the column; the finite element used was a quadrilateral element with four nodes (QUAD4) and four Gaussian points (see Fig. 12(b)); ii) second with a mesh for RVE which is analyzed by the

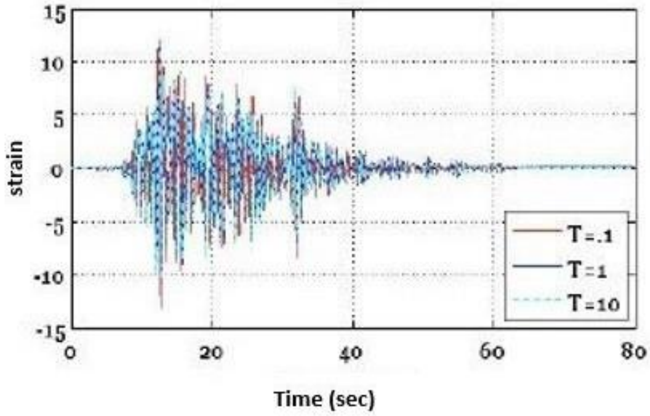

Fig. 13 Time deformation curve increasing relaxation time

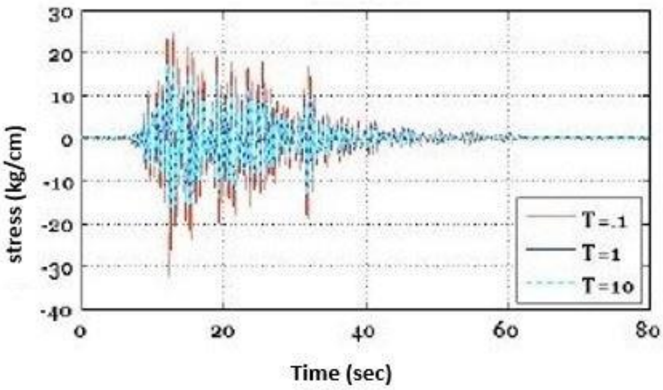

Fig. 14 Stress time curve increasing relaxation time

Homogenization Method (see Fig. 12(a)); in this case, we used viscoelastic material for cement and elastic material for aggregate, with the same finite element used as in the first analysis. Finally, a comparison of the behavior of the two previous analyzes is presented. In all the models, the boundary conditions of the column were: constrained at the level of lower nodes and with imposed displacements caused by the earthquake at the level of upper region.

3.2.1 Analysis of viscoelastic parameters with rectangular mesh

In this analysis we used viscoelastic material, intending to study the viscosity parameters that can affect the behavior of the column. The mesh is presented in Fig. 12(b). First, the value μ_1=0.7 of the Prony series was kept constant, and the time relaxation parameter was changing between the values of .1, 1, and 10 as follows.

Fig. 15 shows the effects of varying the relaxation parameter over time of the material. It can be seen that by reducing this value, the hysteresis loops of the model increase their width and thus the energy dissipation.

Below is a variation of the relaxation time parameter for viscoelastic material in the range of .1 to 1 with increments of .2 where there is an considerable dissipation.

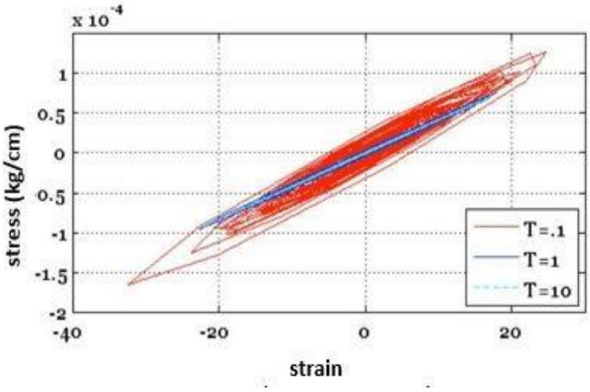

Fig. 15 Stress-strain curve increasing relaxation time

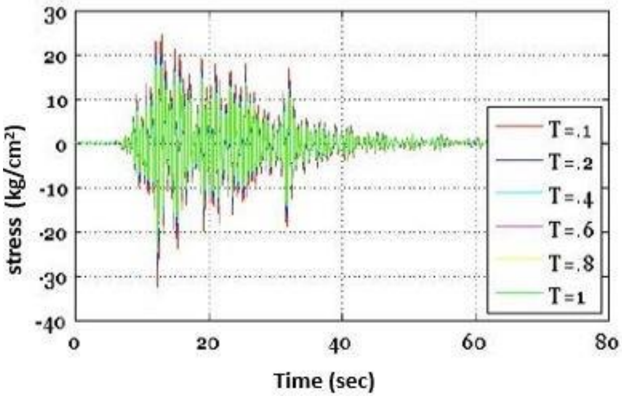

Fig. 16 Stress-time curve variation of relaxation time in the range of .1 to 1

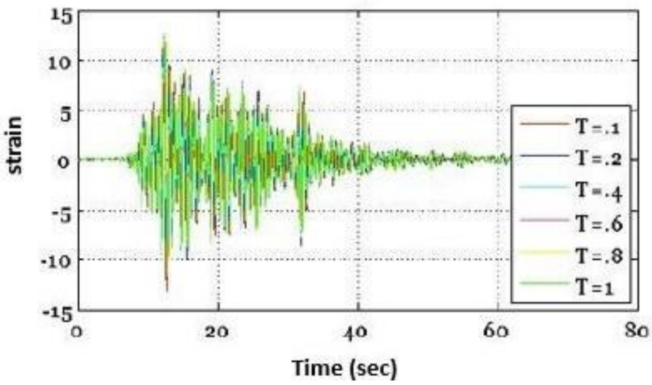

Fig. 17 Strain-time curve variation of relaxation time in the range of .1 to 1

3.2.2 Mesh with RVE

The analysis of the mesh with viscoelastic material of the most unfavorable column 5c (see Fig. 9) is presented in the flowing paragraphs. The mesh is with RVE (see Fig. 12(a)) and sizes vary in the following proportions NxM (see Fig. 6) 5×10, 10×20, 10×50 and 15×50. In Fig. 21 we can see

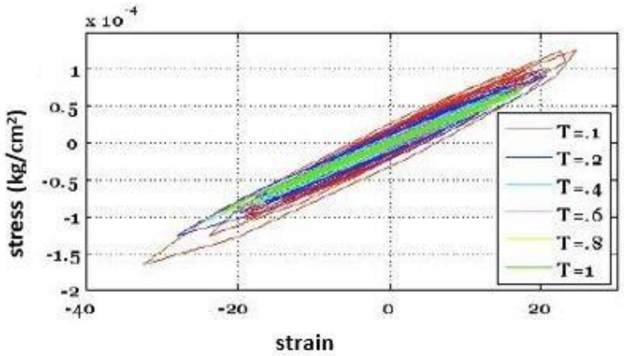

Fig. 18 Stress-strain curve variation of relaxation time in the range of .1 to 1

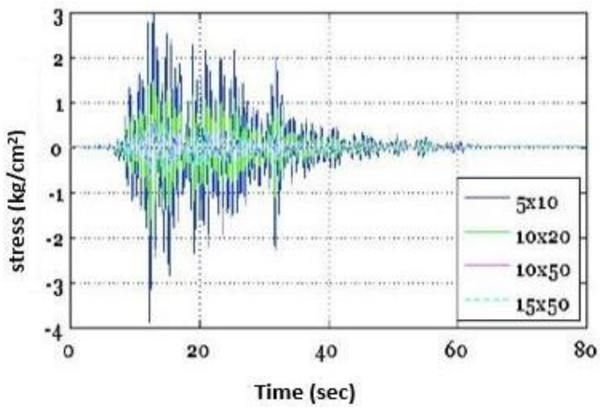

Fig. 19 Stress time curve

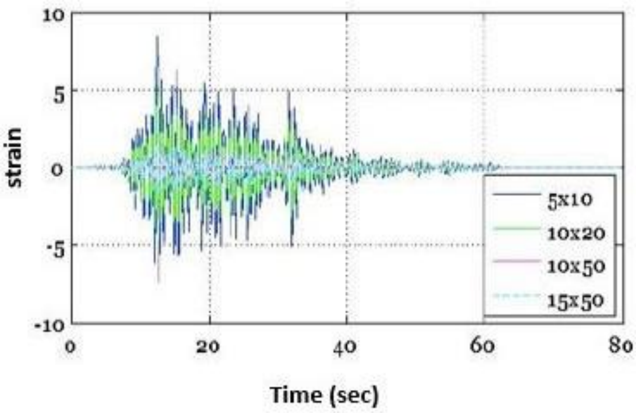

Fig. 20 Time strain curve

that from the 10×50 mesh the stresses and strains are practically the same.

3.2.3 Comparison of the two types of mesh

A comparison of the results obtained for column 5C is presented. On one side the column with a

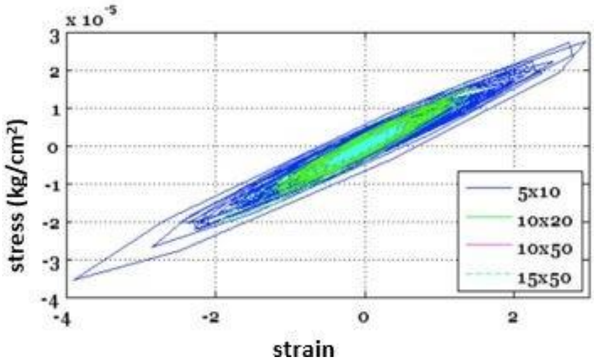

Fig. 21 Stress strain curve

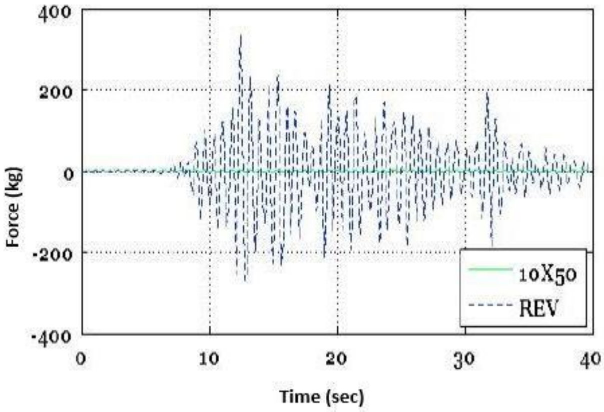

Fig. 22 Time force curve

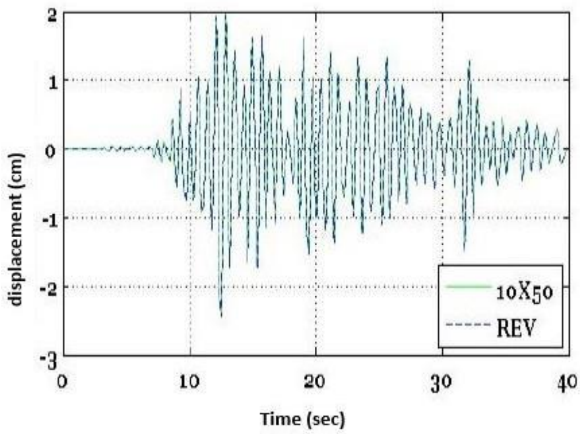

Fig. 23 Time displacement curve

10×50 mesh with rectangular elements having viscoelastic properties, and on the other side with a mesh based on the RVE elaborated in chapter 2. In this case, the mesh has elastic properties in the part that corresponds to the coarse aggregate and viscous properties for cement and sand. In Fig. 24

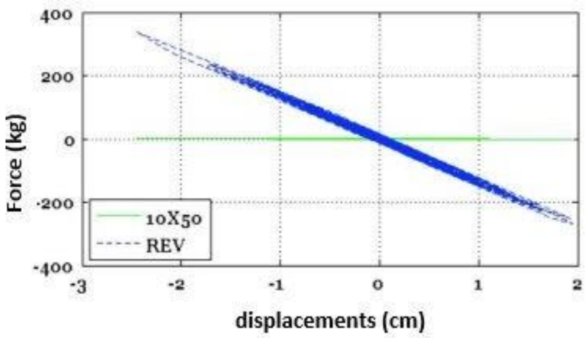

Fig. 24 Force displacement curve

we can see how the column meshed with the RVE presents broader hysteretic cycles than the one created with a single material.

4. Conclusions

In this paper, we have applied homogenization methods by using the classical representative volume element approach in order to study viscoelastic behavior of concrete. This strategy belongs intrinsically to multiscale approach with scale separation. Regarding the choice of the most appropriate multiscale strategy, it can be concluded that concrete materials can be studied at the mesoscale (with visible separation between aggregate and cement) in order to determine their behavior at the macro-scale.

The homogenization procedure can be successfully used in order to facilitate the determination of the structure response and give better results for homogenized structure properties. Both macro-scale and micro-scale models can successfully be analyzed by using the finite element method, where data transfer is possible between scales in order to provide an efficient algorithm similar to those used for parallel computations.

Regarding homogenization strategies, we can conclude that the main advantage of using homogenized materials pertains to ability to account more precisely for the material characteristics of each phase (aggregate versus cement). It is thus much easier providing the corresponding mixture properties that are representative of the structure heterogeneity (which cannot be included for homogeneous material) by using the correct percentage for each material phase to provide the characteristics of the homogenized material.

We showed that quite reliable values of representative properties could be obtained through such homogenization, both for elastic and for viscous response, in order to characterize the heterogeneous materials with the homogenization theory through an RVE on the micro-scale, and successfully incorporate into the macro-scale. The resulting damping coefficient values are closer to reality when they are estimated with multiscale methods.

Regarding the viscoelastic analysis, we can conclude the following: the viscoelastic behavior depends on the relaxation time of the material, which directly affects the amount of dissipated energy. In this work, the relaxation time from which the material presents its greatest contribution to the energy dissipation was detected, along with the corresponding maximum value that can be determined iteratively.

Acknowledgments

The research described in this paper was financially supported by the Chair de Mecanique UTC, Regional government HdF, Institut Universitaire de France (IUF), and CONACYT Mobility Scholarship Program of Mexico.

References

Abbas, S., Mohsen, G. and Daryush, K. (2014), "Equivalent modal damping ratios for non-classically damped mixed concrete-steel buildings with transitional storey", *Struct. Eng. Mech.*, **50**(3), 383-401. http://doi.org/10.12989/sem.2014.50.3.383.

Benkemoun, N., Ibrahimbegovic, A. and Colliat, J.B. (2012), "Anisotropic constitutive model of plasticity capable of accounting for details of meso-structure of two-phase composite material", *Comput. Struct.*, **90-91**, 153-162. https://doi.org/10.1016/j.compstruc.2011.09.003.

Chopra, A.K. (2014), *Dynamics of Structures Theory and Applications to Earthquake Engineering*, 4th Edition, Pearson.

Clough, W. and Penzien, J. (1995), *Dynamics of Structures*, 3rd Edition, McGraw-Hill.

Dujc, J., Brank, B. and Ibrahimbegovic, A. (2010), "Multi-scale computational model for failure analysis of metal frames that includes softening and local buckling", *Comput. Meth. Appl. Mech. Eng.*, **199**, 1371-1385. https://doi.org/10.1016/j.cma.2009.09.003.

Hajdo, E., Mejia Nava, R.A., Imamovic, I. and Ibrahimbegovic, A. (2021), "Linearized instability analysis of frame structures under non-conservative loads: Static and dynamic approach", *Coupl. Syst. Mech.*, **10**, 79-102. http://doi.org/10.12989/csm.2021.10.1.079.

Hautefeuille, M., Colliat, J.B., Ibrahimbegovic, A., Matthies, H. and Villon, P. (2012), "Multiscale approach to modeling inelastic behavior with softening", *Comput. Struct.*, **94**, 83-95.

Ibrahimbegovic, A. (2009), *Nonlinear Solid Mechanics: Theoretical Formulations and Finite Element Solution Methods*, Springer, Berlin.

Ibrahimbegovic, A. and Ademovic, N. (2019), *Nonlinear Dynamics of Structures Under Extreme Transient Loads*, CRC Press.

Ibrahimbegovic, A. and Markovic, D. (2003), "Strong coupling methods in multi-phase and multi-scale modeling of inelastic behavior of heterogeneous structures", *Comput. Meth. Appl. Mech. Eng.*, **192**, 3089-3107. https://doi.org/10.1016/S0045-7825(03)00342-6.

Ibrahimbegovic, A. and Mejia-Nava, R.A. (2021), "Heterogeneities and material-scales providing physically-based damping to replace Rayleigh damping for any structure size", *Coupl. Syst. Mech.*. (in Press)

Ibrahimbegovic, A. and Papadrakakis, M. (2010), "Multiscale and mathematical aspects in solid and fluid mechanics", *Comput. Meth. Appl. Mech. Eng.*, **199**, 21-22.

Ibrahimbegovic, A., Davenne, L., Markovic, D. and Dominguez, N. (2014), "Performance based earthquake-resistant design: Migrating towards nonlinear models and probabilistic framework", *Performance Based Seismic Engineering Vision for Earthquake Resilient Society*, Ed. M. Fischinger, Springer.

Ibrahimbegovic, A., Niekamp, R., Kassiotis, C., Markovic, D. and Matthies, H. (2014), "Code-coupling strategy for efficient development of computer software in multiscale and multiphysics nonlinear evolution problems in computational mechanics", *Adv. Eng. Softw.*, **72**, 8-17. https://doi.org/10.1016/j.advengsoft.2013.06.014.

Kim, J.J., Fan, T. and Reda Taha, M.M. (2011), "A homogenization approach for uncertainty quantification of deflection in reinforced concrete beams considering microstructural variability", *Struct. Eng. Mech.*, **38**(4), 503-516. http://doi.org/10.12989/sem.2011.38.4.503.

Lee, H.J., Kim, Y.R. and Kim, S.H. (1999), "Viscoelastic constitutive modeling of asphalt concrete with growing damage", *Struct. Eng. Mech.*, **7**(2), 225-240. http://doi.org/10.12989/sem.1999.7.2.225.

Marenic, E., Soric, J. and Ibrahimbegovic, A. (2012), "Adaptive modelling in atomistic-to-continuum

multiscale methods", *Int. J. Serbian Soc. Comput. Mech.*, **6**, 169-198.
Markovic, D., Niekamp, R., Ibrahimbegovic, A., Matthies, H.G. and Taylor, R.L (2005), "Multi-scale modeling of heterogeneous structures with inelastic constitutive behavior. Part I: Mathematical and physical aspects", *Int. J. Eng. Comput.*, **22**, 664-683. https://doi.org/10.1108/02644400510603050.
Mejia Nava, R.A., Ibrahimbegovic, A. and Lozano, R. (2020), "Instability phenomena and their control in statics and dynamics: Application to deep and shallow truss and frame structures", *Coupl. Syst. Mech.*, **9**, 47-62. https://doi.org/10.12989/csm.2020.9.1.047.
Niekamp, R., Markovic, D., Ibrahimbegovic, A., Matthies, H.G. and Taylor, R.L (2009), "Multi-scale modeling of heterogeneous structures with inelastic constitutive behavior. Part II: Software coupling and implementation aspects", *Int. J. Eng. Comput.*, **26**, 6-28. https://doi.org/10.1108/02644400910924780.
Pham, B.H., Brancherie, D., Davenne, L. and Ibrahimbegovic, A. (2013), "Stress-resultant models for ultimate load analysis of reinforced concrete frames and its multi-scale parameter estimates", *Comput. Mech.*, **51**, 347-360. https://doi.org/10.1007/s00466-012-0734-6.
Rukavina, I., Ibrahimbegovic, A., Do, X.N. and Markovic, D. (2019), "ED-FEM multi-scale computation procedure for localized failure", *Coupl. Syst. Mech.*, **8**, 117-127. http://dx.doi.org/10.12989/csm.2019.8.2.117.
Rukavina, T., Ibrahimbegovic, A. and Kozar, I. (2019), "Multi-scale representation of plastic deformation in fiber-reinforced materials: application to reinforced concrete", *Latin Am. J. Solid. Struct.*, **25**, 1-11.
Sarfaraz, M.S., Rosic, B., Matthies, H.G. and Ibrahimbegovic, A. (2020), "Bayesian stochastic multi-scale analysis via energy consideration", *Adv. Model. Simul. Eng. Sci.*, **7**, 50-85. https://doi.org/10.1186/s40323-020-00185-y.
Silvestri, S., Trombetti, T. and Ceccoli, C. (2003), "Inserting the mass proportional damping (MPD) system in a concrete shear-type structure", *Struct. Eng. Mech.*, **16**(2), 177-193. http://doi.org/10.12989/sem.2003.16.2.177.
Taylor, R.L. (2008), *Version 8.2 Theory Manual FEAP*.
Ugur, A., Baris, B. and Yalin, A. (2014), "Earthquake stresses and effective damping in concrete gravity dams", *Earthq. Struct.*, **6**(3), 251-266. http://doi.org/10.12989/eas.2014.6.3.251.
Xiaoran, L., Yuanfeng, W. and Li, S. (2014), "Damping determination of FRP-confined reinforced concrete columns", *Comput. Concrete*, **14**(2), 163-174. http://doi.org/10.12989/cac.2014.14.2.163.
Yonggang, Z., Yonghong, W. and Yuanyuan, Z. (2021), "Computer simulation for stability analysis of the viscoelastic annular plate with reinforced concrete face sheets", *Comput. Concrete*, **27**(4), 369-383. http://doi.org/10.12989/cac.2021.27.4.369.